ADVANCED MATERIALS

DOI: 10.1002/adma.200601412

Intracellular Trafficking of Carbon Nanotubes by Confocal Laser Scanning Microscopy**

By *Lara Lacerda*, *Giorgia Pastorin*, *David Gathercole*, *Joanna Buddle*, *Maurizio Prato*, *Alberto Bianco*, and *Kostas Kostarelos**

We describe a simple methodology to study the interactions between ammonium-functionalized single-walled carbon nanotubes (SWNT-NH^{3+}s), free of fluorescent labels, with mammalian cells. We exploit the intrinsic UV-vis luminescence of these nanostructures by using confocal laser scanning microscopy (CLSM) with established and widely used optics. Tracking the luminescence signal of SWNT-NH^{3+}s with CLSM demonstrates that these nanotubes can traffick intracellularly, and elucidates in 3D their perinuclear localization. Imaging of SWNT-NH^{3+} luminescence is a powerful tool that allows for facile and widespread study of the interactions between nanotubes and living tissues in vitro and in vivo.

Recently, the development of carbon nanotubes (CNTs) as delivery systems for nucleic acids,[1–5] proteins,[6,7] and drug molecules[8,9] into mammalian cells and living tissues has attracted much attention. Previous reports have also studied the toxicological impact and safety profile of carbon nanomaterials following cellular uptake,[10,11] indicating that a higher degree of CNT functionalization leads to a dramatic reduction in toxic effects.[12]

[*] Dr. K. Kostarelos, L. Lacerda, Dr. D. Gathercole
Nanomedicine Laboratory
Centre for Drug Delivery Research and Confocal Microscopy Unit
The School of Pharmacy
University of London
29–39 Brunswick Square, London WC1N 1AX (UK)
E-mail: kostas.kostarelos@pharmacy.ac.uk
Dr. G. Pastorin, Dr. A. Bianco
CNRS, Institut de Biologie Moléculaire et Cellulaire
Laboratoire d'Immunologie et Chimie Thérapeutiques
67084 Strasbourg (France)
J. Buddle
Institute of Child Health
University College London
30 Guilford Street, London WC1N 1EH (UK)
Prof. M. Prato
Dipartimento di Scienze Farmaceutiche
Università di Trieste
34127 Trieste (Italy)

[**] This work was financially supported by the School of Pharmacy, University of London, CNRS, the Agence National de la Recherche (ANR-05-JCJC-0031-01), the University of Trieste, and MIUR (PRIN 2004, prot. 2004035502). L.L. acknowledges the Portuguese Foundation for Science and Technology (FCT/MCES) for the award of a Ph.D. fellowship (Ref.: SFRH/BD/21845/2005). G.P. is grateful to French Ministry for Research and New Technologies for a postdoctoral fellowship (GenHomme Network 2003). Supporting Information is available online from Wiley InterScience or from the author.

Perhaps the most commonly used methodology to study the effectiveness of delivery systems carrying biologically active molecules intracellularly is by fluorescence microscopy techniques.[13] CLSM is a widely used optical sectioning microscopy technique that offers fluorescence imaging of thin slices of specimens several micrometers in depth.[14] This powerful technique allows us to remove the contribution of background fluorescence in each *z*-section and to digitally construct 3D images of biological specimens.[14] The application of CLSM to visualize CNT interactions within living biological matter has not been previously shown, and is thought to help advance our understanding of the intracellular transport properties of CNTs.

Previous studies have used different types of fluorescently labeled CNT conjugates to allow their visualization by fluorescence microscopy following interaction with mammalian cells. However, the chemical processing of the CNT graphene sidewalls required to achieve conjugation with fluorescent probes and the presence of the bulky fluorescent molecules themselves, such as fluorescein isothiocyanate (FITC), at the surface of the nanotubes alters their surface properties, and may interfere with nanotube binding, uptake, and intracellular trafficking into mammalian cells. Therefore, methodologies that allow facile study of the interactions between cells and CNTs free of fluorescent probes are needed.

We have been developing delivery systems based on SWNT-NH^{3+}s prepared, as previously described,[15] by the 1,3-dipolar cycloaddition of azomethine ylides. This chemical functionalization methodology not only allowed the development of water-soluble CNTs, but also improved the dissociation of aggregates (bundles) of nanotubes in solution. Ammonium groups are some of the simplest groups that can be introduced around the tips and sidewalls of the nanotubes (Fig. 1a). In agreement with others,[16–19] we have reported that the functionalization of CNTs (single- and multiwalled) via the 1,3-cycloaddition reaction results in covalently linked aliphatic appendages terminated in NH_3^+ (or other chemical moieties), and leads to the emergence of a luminescence signal with characteristic broad 395/485 nm (excitation/emission) peaks detected by fluorescence spectrophotometry.[20] Moreover, SWNT-NH^{3+}s have been shown to be able to effectively deliver plasmid DNA (pDNA) intracellularly, leading to upregulation of gene expression compared with pDNA alone.[1]

In an attempt to visualize whether SWNT-NH^{3+}s alone are capable of binding, uptake, and intracellular trafficking inside

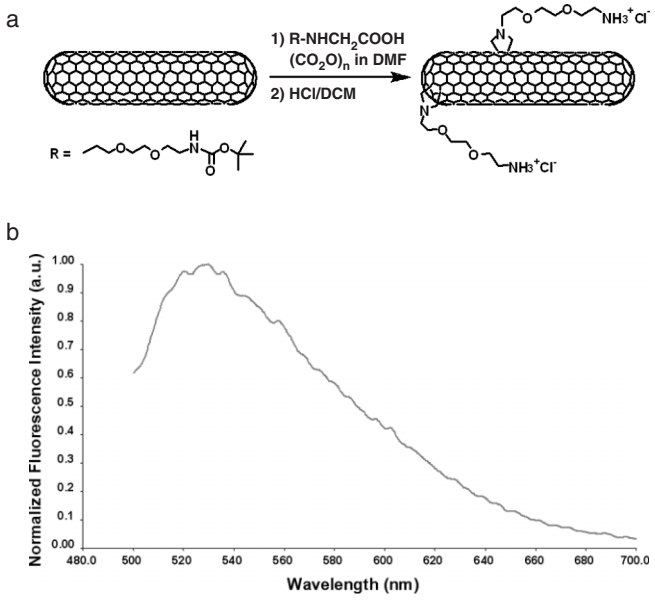

Figure 1. a) Functionalization and structure of SWNT-NH^{3+}s. b) Fluorescence spectrum of an aqueous solution of SWNT-NH^{3+}s (150 μg mL^{-1}) excited at 488 nm.

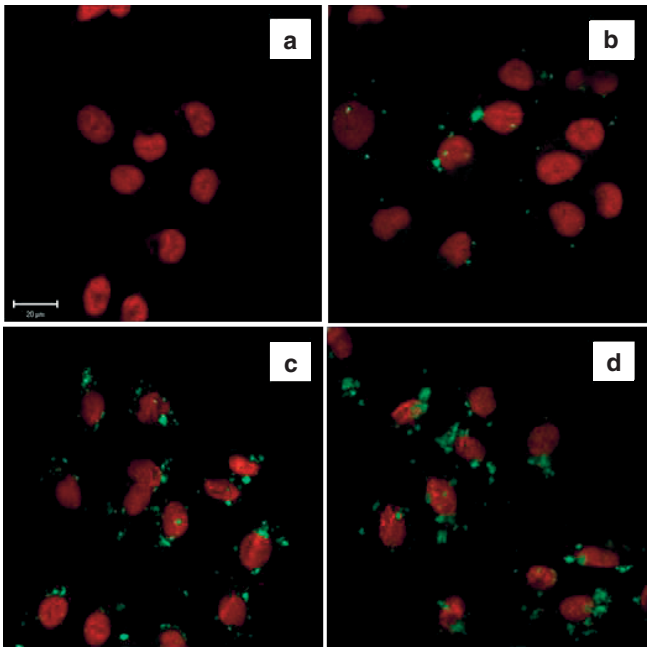

Figure 2. Confocal images of A549 cells incubated for 2 h with different doses of SWNT-NH^{3+}s (green). a) A549 cells alone. b) 5 μg SWNT-NH^{3+}s. c) 25 μg SWNT-NH^{3+}s. d) 50 μg SWNT-NH^{3+}s. Cellular nuclei are counterstained red by using propidium iodide (PI). (Scale bar: 20 μm.)

living mammalian cells, we have used CLSM with standard optics. The instrumentation employed (see Experimental) to detect the interaction of SWNT-NH^{3+}s with mammalian cells consists of a CLSM setup widely employed in molecular and cellular biology. Standard light source and excitation/emission filters for green fluorophores were used to detect the SWNT-NH^{3+} signal. Utilization of the intrinsic SWNT-NH^{3+} luminescence allowed the intracellular visualization and tracking of the SWNT-NH^{3+} signal.

Excitation of SWNT-NH^{3+}s at 488 nm, the same wavelength as the argon laser used in the CLSM imaging studies, produces a fluorescence spectrum with a single peak at 530 nm (Fig. 1b). SWNT-NH^{3+}s were subsequently allowed to interact with planar cell cultures of the lung epithelial cell line A549 for 2 h at 37 °C at increasing concentrations, namely 5, 25, and 50 μg in 100 μL of serum-free media. The cells were imaged after fixation and counterstaining of the nuclei with propidium iodide (PI; red). Following this protocol, the detected green signal increased in proportion to the concentration of SWNT-NH^{3+}s allowed to interact with the cells (Fig. 2). This confirmed that the green signal visualized by CLSM correlates with the concentration of SWNT-NH^{3+}s added to the cells, and that the intracellular fluorescence signal detected follows a SWNT-NH^{3+} dose response. Therefore, as more SWNT-NH^{3+}s were added to the cell cultures, more were taken up intracellularly. Identical results were obtained from CLSM imaging studies using the Chinese Hamster Ovary (CHO) cell line (data not shown).

The SWNT-NH^{3+}s post-functionalization were more individualized than nonfunctionalized nanotubes in aqueous-based solutions. To further investigate the nanotube aggregates observed intracellularly in Figure 2, SWNT-NH^{3+}s were incubated in the absence of cells for 2 h at 37 °C in two different media: water only and serum-free cell medium. Both samples were fixed, stained (as if they contained cells), and imaged under the same optical setup as in the experiments using cells. The SWNT-NH^{3+}s in double-distilled water were imaged as well-dispersed small aggregates that adhered to the bottom of the cover slip, whereas large SWNT-NH^{3+}s aggregates, similar to those detected intracellularly in Figure 2, were obtained when the nanotubes were incubated in the serum-free cell medium (see Supporting Information, Fig. S1). Our previous investigations[17] have also indicated that the low pH is not responsible for changes in the aggregation state of SWNT-NH^{3+}s. Therefore, Figure S1 indicated that SWNT-NH^{3+} aggregation was dependent on the medium, with enhanced aggregation detected for SWNT-NH^{3+}s in serum-free cell-culture medium.

To confirm that the observed SWNT-NH^{3+} luminescence signal (green) was located intracellularly (at the same axis as the nuclear stain) instead of adsorbing onto the cell surface, and identify the exact intracellular location following their internalization, multilabeling CLSM studies were performed. After incubation of SWNT-NH^{3+}s with A549 cells for 2 h at 37 °C (5 % CO_2), the cells were fixed, the cell membranes stained (in red) with a solution of wheat-germ agglutinin conjugated with tetramethylrhodamine (WGA-TRITC), and the nuclei counterstained (in blue) with a solution of TO-PRO 3 (Molecular Probes, Invitrogen) and RNase A. The CLSM optical setup was in multichannel mode, and again the SWNT-NH^{3+} green signal was clearly visualized (Fig. 3). The SWNT-NH^{3+}s were found intracellularly, at the perinuclear region within a short period of 2 h following addition onto the cell

ADVANCED MATERIALS

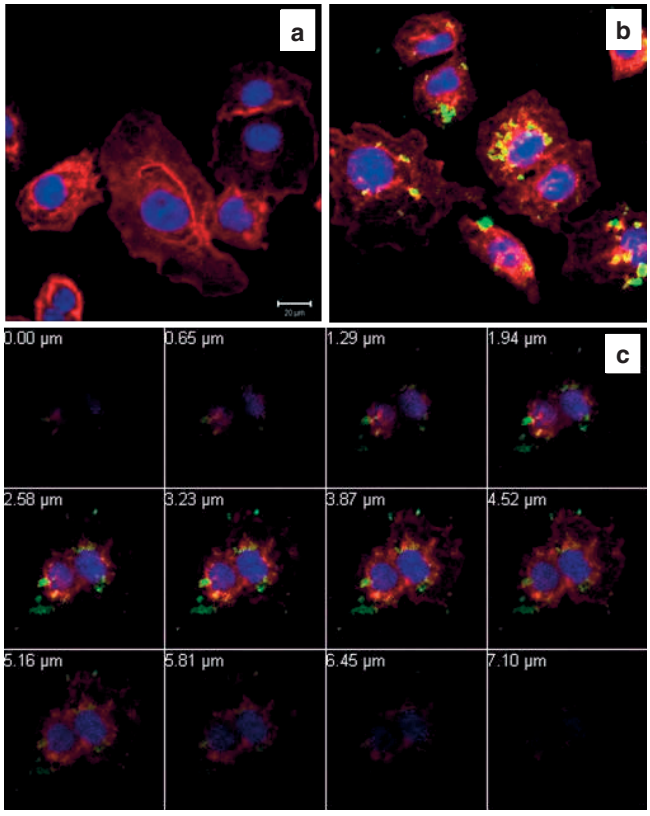

Figure 3. Multiple stain confocal images of A549 cells. a) incubated for 2 h (37 °C, 5 % CO_2) in the absence of SWNT-NH^{3+}s (control); b) in the presence of 20 µg of SWNT-NH^{3+}s. (Scale bar: 20 µm.) c) *z*-stack imaging data obtained from the preparation were A549 cells were incubated with 20 µg of SWNT-NH^{3+}s. Cellular membranes are stained in red with WGA-TRITC and nuclei are counterstained in blue with TO-PRO 3.

cultures (Fig. 3b). This was thought to directly indicate that SWNT-NH^{3+}s traffic intracellularly, leading to perinuclear accumulation. The nanotubes seemed to be able to travel intracellularly around the cell nuclei throughout the cell cultures in our studies, in what appeared to be perinuclear accumulation of multiple nanotube aggregates.

The CLSM imaging data collected as a series of the *z* optical axis (*z*-stack) indicated that the intracellular and perinuclear localization of the SWNT-NH^{3+} signal was at the same plane of focus as the nuclear stain (Fig. 3c). This verified that the SWNT-NH^{3+} luminescence signal was indeed localized within the cell. An animated reconstruction of the *z*-stack imaging data (Fig. 3c) can be found online (see Supporting Information Videoclip). We have observed such perinuclear localization of SWNT-NH^{3+}s consistently throughout our CLSM studies using multiple cell types (data not shown). Such observations make SWNT-NH^{3+}s extremely promising candidates for intracellular transport of biologically active molecules,[1,2] by confirming that SWNT-NH^{3+}s themselves are capable of internalizing and trafficking within cells. Furthermore, at a dose of up to 500 µg mL^{-1} of SWNT-NH^{3+}s used in CLSM studies no cell detachment or cell death was observed microscopically.

To further assess cell viability following SWNT-NH^{3+} internalization and intracellular trafficking, a fluorescence-activated cell sorter (FACS) study was carried out using PI and Annexin V-FITC cellular staining. This assay allows the detection and quantification of healthy, apoptotic, and necrotic cells within a cell population. No differences were found between the control (untreated) cell cultures and the cells that interacted with increasing doses of SWNT-NH^{3+}s (Fig. 4a–c). In addition, PI allowed us to confirm cellular membrane integrity following interaction with SWNT-NH^{3+}s. By analyzing the flow cytometry histograms of PI staining, no shift was observed between the histograms of the different samples (see Fig. S2). Lastly, the cells were studied 24 h post-incubation with SWNT-NH^{3+}s, and again no differences were found between the untreated and treated cells (see Fig. S3). Thus, we confirmed that the incubation and the cellular internalization of SWNT-NH^{3+}s have not caused any damage on the plasma membrane within 24 h post-incubation at the doses used in this study. These results are in complete agreement with recently reported findings that describe the absence of toxic effects of SWNT-NH^{3+}s on immunocompetent cells.[21]

This is the first study to report that intracellular trafficking of SWNT-NH^{3+}s can lead to their accumulation in the perinuclear region of mammalian cells, free of any misinterpretations that may be introduced by coating or conjugating fluorescently labeled macromolecules onto the surfaces of CNTs. Previous studies reported the uptake of CNTs by cells; however, all such studies were performed by using CNTs functionalized with fluorescently labeled peptides[6] or pristine nanotubes coated with various macromolecules, such as proteins[7] and polymers.[22,23] All such macromolecules that are at the surface of the CNTs will dramatically alter the observed interactions with cells. It is also demonstrated that imaging of SWNT-NH^{3+}s is feasible by using protocols of multiple fluorescent staining of cellular compartments. No direct evidence of CNTs intracellular trafficking leading to perinuclear localization has previously been offered by using conventional optics and CLSM instrumentation. Some of the previously reported studies[22–24] have described the utilization of the intrinsic IR fluorescence of pristine SWNTs (coated with surfactants or polymers) to image and study CNTs intracellularly, however the instrumentation and technique used is complex and not widely used, particularly in cell-biology-related investigations.

Monitoring SWNT-NH^{3+}s, not coated with biopolymers or other macromolecules, is considered of paramount importance when interactions with components of the biological milieu and living cell compartments are involved. The presence of macromolecules commonly used to achieve the solubilization of CNTs determines the surface character of these nanostructures, and the ensuing interactions with living cells and tissues. The methodology presented herein to image and monitor the intracellular processes of uncoated nanotubes using the CLSM technique is expected to offer a widely usable tool, which will further elucidate the ensuing intracellular transport mechanisms of CNTs.

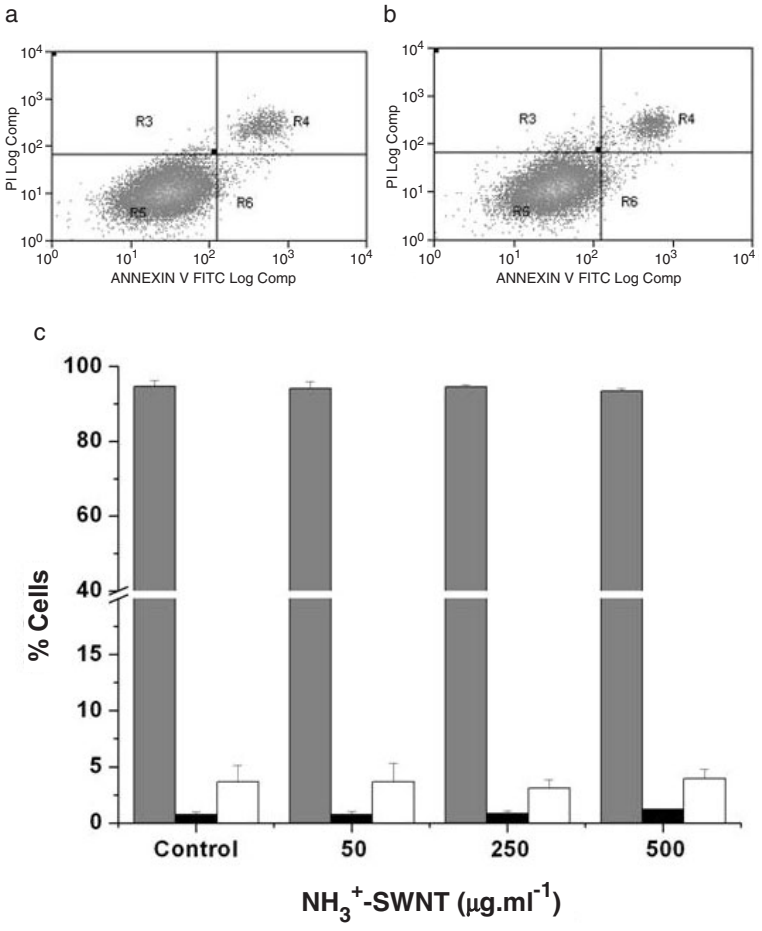

Figure 4. Flow cytometry (Propidium Iodide–Annexin V Assay) analysis of A549 cells incubated for 2 h (37 °C, 5 % CO_2) a) without SWNT-NH^{3+}s (control) and b) in the presence of SWNT-NH^{3+}s (500 μg mL^{-1}). c) Percentage of live (grey bars), apoptotic (black bars) and late apoptotic/necrotic cells (white bars) after 2 h incubation (37 °C, 5 % CO_2) with different concentrations of SWNT-NH^{3+}s.

Experimental

Functionalization of Carbon Nanotubes: Purified single-walled carbon nanotubes (SWNTs) were purchased from Carbon Nanotechnologies Inc. (CNI Grade/Lot #: R0496; Houston, USA). According to the supplier the median diameter of SWNT was ca. 1 nm, tube lengths were between 300 and 1000 nm, and the tube ends were closed.

Water soluble single-walled carbon nanotubes functionalized with ammonium groups (SWNT-NH^{3+}s) were synthesized by the 1,3-dipolar cycloaddition reaction methodology and characterized as described elsewhere [6,25]. The concentration of available functional groups on the SWNT surface was determined by using the quantitative Kaiser test as 0.6 mmol per gram of material [26]. A stock solution was prepared by hydration in deionized water and brief bath sonication (45 kHz) at a concentration of 6 mg mL^{-1}. The stock solution was kept at 4 °C until needed, and all further dilutions were prepared with deionized water.

Fluorescence Spectrophotometry: The fluorescence spectra for a 150 μg mL^{-1} aqueous solution of SWNT-NH^{3+}s were obtained with a LS-50B spectrophotometer (Perkin Elmer). The excitation wavelength used corresponded to the common confocal line used to visualize yellow/green fluorophores (488 nm). The fluorescence spectra presented were normalized such that the maximum peak of the spectrum was equivalent to 1.0 arbitrary units (a.u.) of fluorescence intensity.

Incubation of Mammalian Cells with SWNT-NH^{3+}s: Human Caucasian lung carcinoma (A549) and Chinese Hamster ovary (CHO) cells were seeded in 16 chambered slides, at a density of 3×10^4 cells per chamber, in Dulbecco's Modified Eagle medium (DMEM) and F12 K Ham's medium (F12 K), respectively. Each of these media was supplemented with 10 % of fetal bovine serum (FBS) and 1 % of antibiotics (penicillin/streptomycin). After incubation overnight at 37 °C in a humidified atmosphere (5 % CO_2), the medium was aspirated off and replaced with fresh serum-free medium. The aqueous solutions of SWNT-NH^{3+}s were introduced on the medium in an appropriate concentration, such that three different doses were reached: 5, 25, and 50 μg. In a fourth chamber (control) only the vehicle of the nanotubes was introduced (deionized water, 20 μL).

Cellular Staining: Following incubation (37 °C, 5 % CO_2) for 2 h the medium was aspirated off, the cells were washed with phosphate buffered-saline (PBS), and fixed with 2 % paraformaldehyde for 1 h at 4 °C. After permeabilization of the cellular membrane with 0.1 % Triton X-100 at 4 °C for 10 min, the cellular nucleus was counterstained in red with a solution of propidium iodide (PI) and RNase A (1 μg mL^{-1} and 100 μg mL^{-1}, respectively) by incubation at 37 °C for 30 min. Finally, the chambers were separated from the slides and the coverslips were mounted with Citifluor AF1. The mounting medium was allowed to be hardened at 4 °C overnight and the preparation was sealed with nail varnish. Alternatively, multiple cellular staining was performed as follows: cell membranes were stained red with a solution of wheat-germ agglutinin conjugated with tetramethylrhodamine (WGA-TRITC, 10 μg mL^{-1}) and the nuclei were counterstained in blue (false color) with a solution of TO-PRO 3 and RNase A (1 μg mL^{-1} and 100 μg mL^{-1}, respectively).

Confocal Laser Scanning Microscopy: Imaging was conducted by using a Zeiss LSM 510 Meta laser scanning confocal microscope. To excite the SWNT-NH^{3+}s and the PI (nucleus counter stain), the argon laser lines of 488 nm (green emission) and 543 nm (red emission), were used, respectively. Band-pass filters were set up, such as 505–530 nm for the green emission signal and 606–670 nm for the red emission signal. In the alternative multiple cellular stain, SWNT-NH^{3+}s were excited with the 488 nm laser line, the WGA-TRITC (cellular membrane stain) with the 543 nm laser line, and the TO-PRO 3 (nuclei counterstain) with the 633 nm laser line. The emission signals passed through the 505–503 nm, 560–615 nm, and 649–799 nm filters, respectively. All images were captured with a Plan-Apochromat 63x/1.4 oil DIC objective and collected in multichannel mode.

Assessment of Cell Viability: A549 cells seeded in 24 well plates were incubated with SWNT-NH^{3+}s in three concentrations: 50, 250, and 500 μg mL^{-1}. In a control chamber was added deionized water to the serum-free DMEM. The nanotubes were allowed to interact with the cells for 2 h at 37 °C in a humidified atmosphere (5 % CO_2). The live–death cell assay was performed with a PI/annexin-V-FITC staining kit (Roche) according to the instructions of the manufacturer at different time points: a) immediately after the incubation with the nanotubes, and b) after replacement of the medium by fresh and complete DMEM and further cell incubation for 24 h following the interaction period. A CyAn ADP flow cytometer (DakoCytomation) was used to analyze between 10 000 and 20 000 cells per sample. All conditions were tested in triplicate.

Received: June 26, 2006
Revised: January 8, 2007
Published online: May 10, 2007

[1] D. Pantarotto, R. Singh, D. McCarthy, M. Erhardt, J. P. Briand, M. Prato, K. Kostarelos, A. Bianco, *Angew. Chem. Int. Ed.* **2004**, *43*, 5242.

[2] R. Singh, D. Pantarotto, D. McCarthy, O. Chaloin, J. Hoebeke, C. D. Partidos, J. P. Briand, M. Prato, A. Bianco, K. Kostarelos, *J. Am. Chem. Soc.* **2005**, *127*, 4388.

[3] Q. Lu, J. M. Moore, G. Huang, A. S. Mount, A. M. Rao, L. L. Larcom, P. C. Ke, *Nano Lett.* **2004**, *4*, 2473.

[4] Y. Liu, D. C. Wu, W. D. Zhang, X. Jiang, C. B. He, T. S. Chung, S. H. Goh, K. W. Leong, *Angew. Chem. Int. Ed.* **2005**, *44*, 4782.

[5] N. W. Kam, Z. Liu, H. Dai, *J. Am. Chem. Soc.* **2005**, *127*, 12 492.

[6] D. Pantarotto, J. P. Briand, M. Prato, A. Bianco, *Chem. Commun.* **2004**, 16.

[7] N. W. Kam, H. Dai, *J. Am. Chem. Soc.* **2005**, *127*, 6021.

[8] G. Pastorin, W. Wu, S. Wieckowski, J. P. Briand, K. Kostarelos, M. Prato, A. Bianco, *Chem. Commun.* **2006**, 1182.

[9] W. Wu, S. Wieckowski, G. Pastorin, M. Benincasa, C. Klumpp, J. P. Briand, R. Gennaro, M. Prato, A. Bianco, *Angew. Chem. Int. Ed.* **2005**, *44*, 6358.

[10] B. J. Panessa-Warren, J. B. Warren, S. S. Wong, J. A. Misewich, *J. Phys. Condens. Matter* **2006**, *18*, S2185.

[11] N. A. Monteiro-Riviere, R. J. Nemanich, A. O. Inman, Y. Y. Wang, J. E. Riviere, *Toxicol. Lett.* **2005**, *155*, 377.

[12] C. M. Sayes, F. Liang, J. L. Hudson, J. Mendez, W. Guo, J. M. Beach, V. C. Moore, C. D. Doyle, J. L. West, W. E. Billups, K. D. Ausman, V. L. Colvin, *Toxicol. Lett.* **2006**, *161*, 135.

[13] Special Issue on Advances in Fluorescence Imaging: Opportunities for Pharmaceutical Sciences, *Adv. Drug Delivery Rev.* **2005**, *57*, 1.

[14] J. A. Conchello, J. W. Lichtman, *Nat. Methods* **2005**, *2*, 920.

[15] V. Georgakilas, K. Kordatos, M. Prato, D. M. Guldi, M. Holzinger, A. Hirsch, *J. Am. Chem. Soc.* **2002**, *124*, 760.

[16] J. E. Riggs, Z. X. Guo, D. L. Carroll, Y. P. Sun, *J. Am. Chem. Soc.* **2000**, *122*, 5879.

[17] S. Banerjee, S. S. Wong, *J. Am. Chem. Soc.* **2002**, *124*, 8940.

[18] D. M. Guldi, M. Holzinger, A. Hirsch, V. Georgakilas, M. Prato, *Chem. Commun.* **2003**, 1130.

[19] Y. Lin, B. Zhou, R. B. Martin, K. B. Henbest, B. A. Harruff, J. E. Riggs, Z. X. Guo, L. F. Allard, Y. P. Sun, *J. Phys. Chem. B* **2005**, *109*, 14 779.

[20] L. Lacerda, G. Pastorin, W. Wu, M. Prato, A. Bianco, K. Kostarelos, *Adv. Funct. Mater.* **2006**, *16*, 1839.

[21] H. Dumortier, S. Lacotte, G. Pastorin, R. Marega, W. Wu, D. Bonifazi, J. P. Briand, M. Prato, S. Muller, A. Bianco, *Nano Lett.* **2006**, *6*, 1522.

[22] P. Cherukuri, S. M. Bachilo, S. H. Litovsky, R. B. Weisman, *J. Am. Chem. Soc.* **2004**, *126*, 15 638.

[23] D. Heller, S. Baik, T. Eurell, M. Strano, *Adv. Mater.* **2005**, *17*, 2793.

[24] D. A. Tsyboulski, S. M. Bachilo, R. B. Weisman, *Nano Lett.* **2005**, *5*, 975.

[25] V. Georgakilas, N. Tagmatarchis, D. Pantarotto, A. Bianco, J. P. Briand, M. Prato, *Chem. Commun.* **2002**, 3050.

[26] V. K. Sarin, S. B. Kent, J. P. Tam, R. B. Merrifield, *Anal. Biochem.* **1981**, *117*, 147.

